

# Mechanical and Thermal Properties of Composite Material and Insulation for a Single Walled Tank for Cryogenic Liquids

Philipp W. Kutz<sup>1,\*</sup>, Frank Otremba<sup>1</sup> and Jan Werner<sup>1</sup>

<sup>1</sup>Bundesanstalt für Materialforschung und -prüfung (BAM), Berlin, 12205, Germany

\*Corresponding author: E-mail: philipp-werner.kutz@bam.de; Tel: (+49) 30 8104 3872

DOI: 10.5185/amlett.2020.011457

This paper describes the testing methods used to determine the thermal properties of insulation materials and mechanical properties of materials used for the load-bearing structure for pressure tanks (up to 4 bar, relative) and cryogenic liquids (LNG,  $-166\text{ }^{\circ}\text{C}$  to  $-157\text{ }^{\circ}\text{C}$  at atmospheric pressure). Goal is to design a transportation tank that does not exceed 4 bars (relative) within 10 h, starting at atmospheric pressure. PUR-foam is a suitable material for the insulation. A 12,5 l small scale tank prototype reached 4 bar (relative) within 87 minutes, which is, regarding the influence of the size, a satisfying result. The mechanical properties change significantly at cryogenic temperatures. The bending modulus is similar at first, but decreases at a certain point by appr. 50 %. However, the maximum stress is much higher and could not be reached within this testing setup.

## Introduction

To reduce the emission of carbon dioxide ( $\text{CO}_2$ ) of combustion engines, liquefied natural gas (LNG) is used as an alternative fuel. It has the lowest  $\text{CO}_2$  emission of all fossil fuels [2]. For transportation, natural gas is cooled down and compressed to LNG, including a volume reduction of approximately 600 to one [3]. LNG is transported via truck, ship or railway for long distances. Double walled stainless steel tanks are used for transportation, which are heavy and expensive. According to [4], single walled tanks are not approved for the transportation of gases below  $-100\text{ }^{\circ}\text{C}$ . For liquids, such as LNG, the tank needs to be double walled and vacuum insulated, following the standard EN 13530. Vacuum is one of the best thermal insulators. At a pressure above 1 mbar, the heat conductivity of a not-moving is not pressure dependent. When lowering the pressure below 1 mbar, the heat conductivity decreases until it reaches a value of zero at  $10^{-3}$  mbar and below [5]. The vacuum insulation between the two walled structure ensures that the LNG stays liquid over the transportation time (boiling point of LNG:  $-166\text{ }^{\circ}\text{C}$  to  $-157\text{ }^{\circ}\text{C}$  at atmospheric pressure [1]). However, these double walled tanks are designed for long transportation times of several days. For delivery traffic, these tanks are oversized and the construction is too complex.

The cryogenic boiling point of LNG causes a high temperature difference between the transported good and the ambient air ( $\Delta T \approx 250\text{ K}$ ). With increasing pressures, the boiling temperature increases as well. The boiling temperature of methane, which is the main component of LNG, increases from  $-161,6\text{ }^{\circ}\text{C}$  at 1000 mbar to  $-137,8\text{ }^{\circ}\text{C}$  at 5000 mbar [6].

This project's goal is to analyze the feasibility and requirements for a single walled design, by carrying out mechanical testing of glass fiber reinforced polymer (GFRP) and a suitable solid layer insulation material under cryogenic conditions. By substitution of stainless steel with GFRP and reducing the double-walled structure to a single-walled design, weight and costs can be reduced. GFRP has excellent mechanical properties and low density. The maximum strength of glass fibers is temperature dependent and reaches the maximum at  $-180\text{ }^{\circ}\text{C}$  and is twice as high as at  $23\text{ }^{\circ}\text{C}$  [7]. Common transportation tanks (20  $\text{m}^3$ , double walled stainless steel) for LNG weigh about 7,8 t [8]. Our project partner, VKA GmbH Schönbrunn, was able to manufacture a transportation tank of the same size, made of GFRP, for drinking water with a weight of 4,5 t. Obviously, the weight of the insulation material is not considered in this comparison, but it underlines how promising the usage of GFRP could be.

Numerical models of the conducted experiments will be set up and can then be used for parameter studies. Goal of this project is to develop a single walled tank structure for the transportation of LNG, which does not exceed an internal pressure of 4 bar relative within 10 h. The structure will consist of an inner liner (leakage), a GFRP structure (load-bearing structure) and the insulation material (reduce heat flow).

## Experimental

Previous tests have shown, that GFRP cannot be used without an additional liner, as leakage occurs due to thermally induced microcracking (Fig. 1).



**Fig. 1.** Leakage throughout the GFRP structure of a small-scale tank prototype at 1 bar (relative) after undergoing several thermal cycles from room temperature to 77 K and back.

Therefore, a steel tank is used as load-bearing structure without additional liner at this point of the project, to prevent leakage. This step is made only to analyze the performance of the insulation material without influence of leaked LN<sub>2</sub>. In future experimental testing, a GFRP structure will be used. The dimensions can be seen in **Table 1**. The volume of LN<sub>2</sub> equals 85% of the total volume, which is the legal regulation for this kind of transportation tank.

**Table 1.** Dimensions of the small-scale tank prototype.

| Volume total [dm <sup>3</sup> ] | Volume LN <sub>2</sub> [dm <sup>3</sup> ] | Volume N <sub>2</sub> [dm <sup>3</sup> ] | PUR-foam insulation [mm] |
|---------------------------------|---|--|--------------------------|
| 12,5                            | 10,6                                      | 1,9                                      | 125                      |

### Thermal properties, Method 1

In the first testing method, the boil-off rate at atmospheric pressure from a small-scale tank prototype is measured to determine the thermal properties and performance. The test setup is shown in **Fig. 2**. Due to the heat flux, LN<sub>2</sub> will evaporate. The gaseous N<sub>2</sub> is piped through a water bath into a beaker. The water bath heats up the gas, to ensure a steady density of the collected gas.

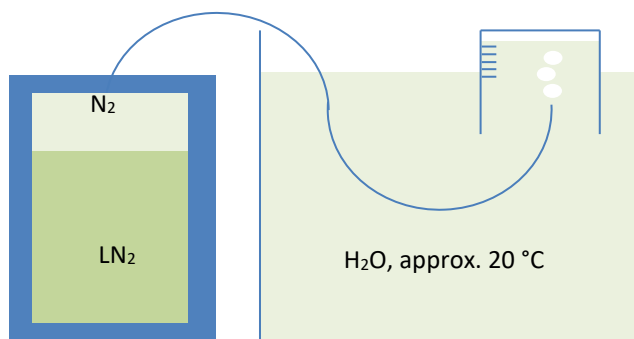


**Fig. 2.** Schematic test setup to determine the boil-off rate at atmospheric pressure.

Water temperature and gas temperature are measured using type k thermocouples (NiCr-Ni) during the experiment. The thermocouples are connected to the measuring instrument “ALMEMO 2890-9” made by Ahlborn. The data is then amplified by a measurement amplifier (“MGCPlus” by HBM) and transferred to a computer running the software “AMR WinControl” for recording. Water temperature is observed for monitoring the experimental conditions. The gas temperature is necessary to calculate the heat influx afterwards. For measuring the gas volume, a calibrated beaker, filled with water and placed upside down in a bowl full of water, is used. A video camera is used to read the gas volume over time.

### Thermal properties, Method 2

The second experiment is conducted to measure the increase of pressure over time up to 4 bar (relative) and the boil-off rate at 4 bar (relative). Therefore, an additional valve is used, which opens automatically if an inner pressure of 4 bar is reached and closes again, so that the pressure is constant at  $4 \pm 0,03$  bar (**Fig. 3**). For opening and closing the valve, a self-written script is being run on a RaspberryPi, where the hysteresis is set to 0,03 bar. The pressure is measured with a pressure transducer (“P3MB” made by HBM, range up to 10 bar) and also recorded with the software “AMR WinControl”. The pressure is measured over time (sensor not shown in **Fig. 3**).

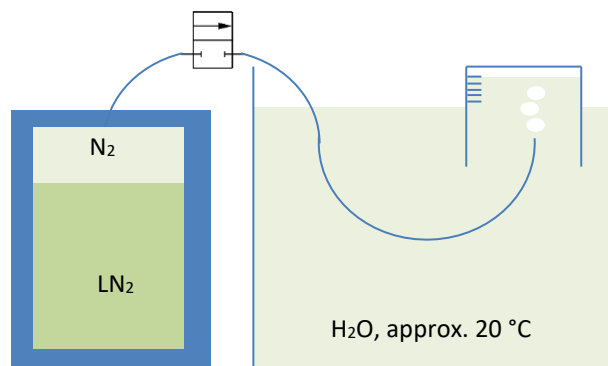


**Fig. 3.** Schematic test setup to determine the increase in pressure and the boil-off rate once 4 bar are reached.

To determine the heat flow, the evaporated mass is calculated by

$$m = \rho * V \quad (1)$$

with

$$\begin{aligned} m &= \text{evaporated mass} \\ \rho &= \text{density of evaporated gas} \\ V &= \text{evaporated Volume} \end{aligned}$$

With the temperature-dependent evaporation enthalpy  $\Delta Q_V$ , the total amount of thermal energy  $E$  can be calculated (2). The ratio of energy to experiment time gives the heat flow  $\dot{Q}$  for the steady state of the system (3).

$$E = m * \Delta Q_V \quad (2)$$

$$\dot{Q} = \frac{E}{t} \quad (3)$$

### Mechanical properties

For the determination of the mechanical properties of GFRP at 77 K, three-point-bending tests are conducted. The specimen are fully submerged in LN<sub>2</sub> during the testing and compared to specimen tested at room temperature. The test setup is thermally decoupled from the testing machine, to prevent damage to the measuring systems (Fig. 4).



Fig. 4. Three-point-bending test stand for cryogenic testing.

The specimen are 180 mm × 30,1 mm × 13,5 mm. They are cut out from a tank wall. The layup is a symmetrical [90°/90°/±60°/90°/±60°/90°]<sub>s</sub> laminate. For both, room temperature and cryogenic temperature, five specimen each were tested. Goal is to determine the bending modulus, the maximum stress and the maximum strain. The bending modulus can be calculated by using (4).

$$E = \frac{L^3}{4bh^3} \left( \frac{\Delta F}{\Delta s} \right) \quad (4)$$

with

$E$  = Bending modulus  
 $L$  = Distance between supports  
 $b$  = specimen's width

$h$  = specimen's thickness

$\Delta F$  = difference of force

$\Delta s$  = difference of deflection

The stress can be calculated by using

$$\sigma = \frac{FL}{bh^2} \quad (5)$$

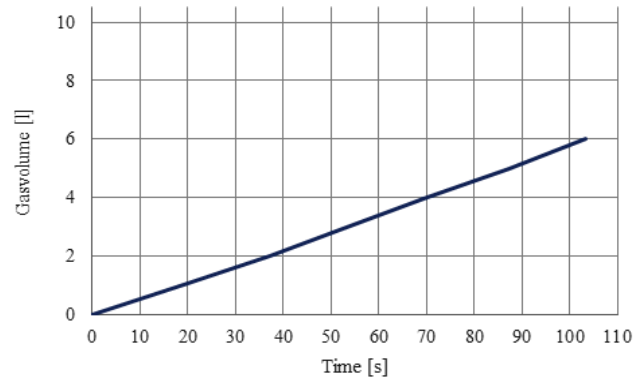


Fig. 5. Boil-off rate at atmospheric pressure.

## Results and discussion

### Thermal properties

Fig. 5 shows the collected gas volume over time at atmospheric pressure. The increase in volume is almost linear. Deviations from the linearity result from inaccuracies of the measuring system. In future experiments it will be substituted by a mass flow measurement system, to gain more precise results. At atmospheric pressure, 6 l of gas were collected over 103 s. The gas temperature was constantly at 18 °C, which gives a density of 1,1745 g/dm<sup>3</sup>. Formula (1) gives an evaporation mass of 7,05 g. For the evaporation of this mass, a heat influx of 13,6 W is calculated.

For the boil-off rate at 4 bar (relative), a heat flow of 10,2 W was calculated (Fig. 6), following the same method as pointed out before. The diagram shows, that 6 l of gas were collected within 100 s. The curve is as well almost linear, having the same inaccuracies as the testing at atmospheric pressure.

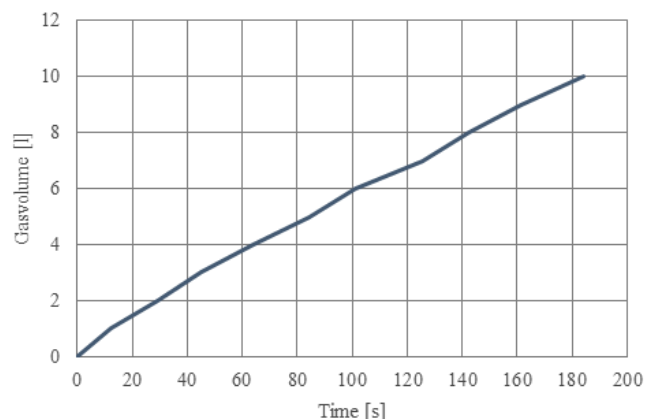


Fig. 6. Boil-off rate at 4 bar (relative).

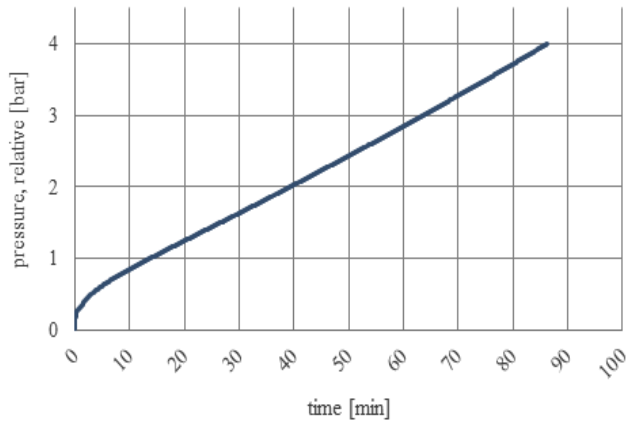


Fig. 7. Increase in pressure over time, PUR-foam insulation.

With this configuration for the insulation, an increase in pressure from atmospheric to 4 bar (relative) was measured in 87 min (Fig. 7). The diagram shows a linear increase in pressure over time.

An analytical parameter study on the influence of the tank volume has shown, that changing the diameter has a massive influence of the increase in pressure over time. In the analytical model, a tank with an inner diameter of 2 m was examined. The insulation had a thickness of 0,1 m with a thermal conductivity of 0,035 W/m<sup>2</sup>K. The tank model had a length of 4 m. The other boundary conditions are not explained more detailed in this paper. In the parameter study, diameters from 1 m to 5 m (0,5 m steps) were examined. The results showed, that there is an almost linear correlation between the diameter and the increase in pressure time. For 1 m, it took approximately 25 until 4 bar (relative) were reached. For a diameter of 2 m, it took approximately 52 h and for 3 m approximately 78 m (Fig. 8, [9]). Taking this analysis into account, the results from the pressure testing can be seen as satisfying.

In future experiments, the correlation of the tank volume to the pressure-increasing-time will be analyzed. The goal is to determine a factor or function that can predict the behavior of a full sized tank after examining a small-scale tank prototype.

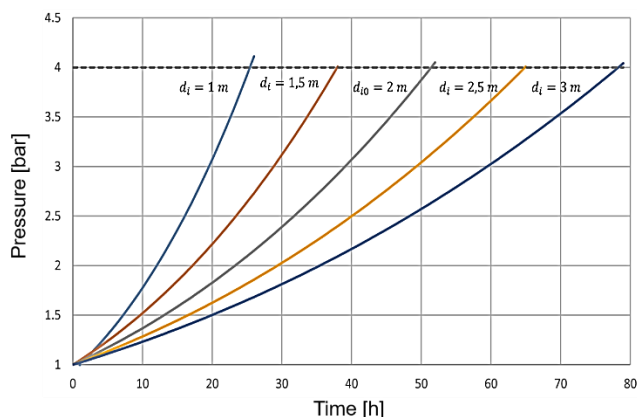


Fig. 8. Analytical calculation of pressure over time for different tank volumes [9].

### Mechanical properties

The three-point-bending test showed a massive difference in terms of mechanical properties regarding the bending modulus, obtained by using (4), and maximum stress. Fig. 9 shows the stress-strain curve for all five specimen tested at room temperature. The typical successive failure of composite material (layer after layer) can be seen clearly. The maximum strain for this testing is at appr. 1,3 % to 1,5 %

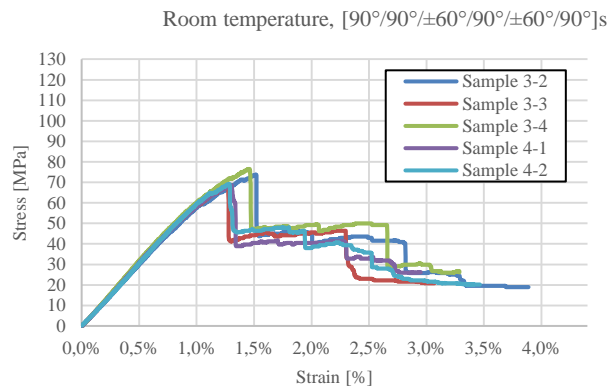


Fig. 9. Stress-strain diagram of 5 specimen tested at room temperature

Table 2 shows the results from the three-point bending test at room temperature. At approximately 60 MPa, the bending modulus reduces slightly. At this point, first failure occurs, most likely at the bottom layer(s), which are strained the most.

Table 2. Results from three-point bending test at room temperature

| Sample | Bending Modulus [MPa] | Max. Stress [MPa] |
|--------|-----------------------|-------------------|
| 3-2    | 6062,48               | 73,81             |
| 3-3    | 6211,84               | 68,39             |
| 3-4    | 6421,14               | 76,48             |
| 4-1    | 6321,85               | 68,66             |
| 4-2    | 6327,97               | 69,16             |

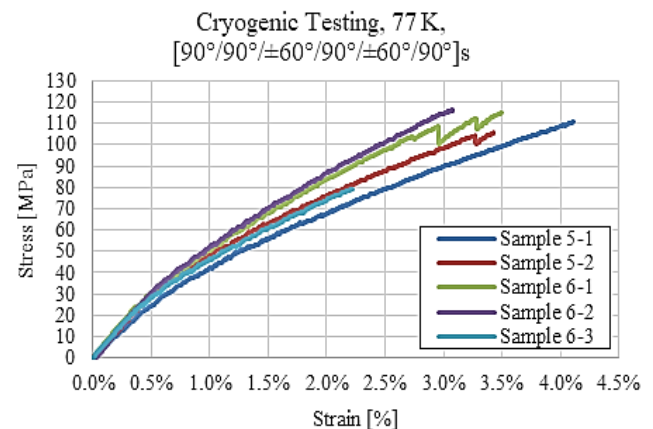


Fig. 10. Stress-strain diagram of five specimen tested at cryogenic temperature.

**Fig. 10** shows the stress-strain curves of five specimen tested at cryogenic temperatures. The decrease of the bending modulus occurs at a lower stress at around 30 MPa. None of the specimen showed complete failure as the maximum stress and strain were much higher than at room temperature and could not be achieved in this testing due to dimensional restriction of the testing setup and exceeded the possible displacement of the mashine.

**Table 3** shows the results from the three-point bending test at cryogenic temperature. Up to 30 MPa, the average bending modulus is at approximately 6.040 MPa. When the load exceeds 30 MPa the bending modulus decreases to an average of approximately 2.800 MPa which is almost 50 % of the starting bending modulus.

**Table 3.** Results from three-point bending test at cryogenic temperature; bending modulus at 0-20 MPa and 60-80 MPa.

| Sample | Modulus 0-20 MPa [MPa] | Modulus 60-80 MPa [MPa] |
|--------|------------------------|-------------------------|
| 5-1    | 5068,38                | 2323,54                 |
| 5-2    | 5901,79                | 2520,00                 |
| 6-1    | 6842,20                | 3253,27                 |
| 6-2    | 5864,28                | 3455,05                 |
| 6-3    | 6537,47                | 2557,46                 |

The higher maximum stress can partly be explained with the mechanisms of stress corrosion cracking of glass fibers (**Fig. 11**). The diffusion of water molecules into the glass structure is almost stopped at cryogenic temperatures, which slows down crack growth. [10] showed, that unidirectional glass-epoxy-specimen achieved much higher maximum stress (1332 MPa to 2050 MPa) and higher elongation at break (2,8 % to 4,3 %) at 77 K compared to room temperature. However, as in this testing a laminate structure with different angles were tested, this effect cannot explain all the differences between the tests at both temperatures.

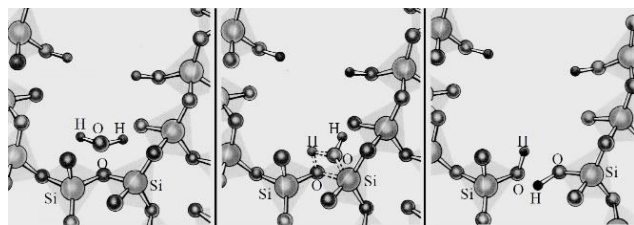


**Fig. 11.** Stress corrosion cracking in glass; diffusion of water into glass structure; [10], adapted from [11].

## Conclusion and outlook

The pretesting underlines the importance of an inner liner to prevent leakage. Thermally induced microcracks led to leakage throughout the GFRP wall. In upcoming testing, an aluminum liner with overwrapped GFRP will be used as a combination of a load-bearing structure and leakage barrier.

The testing of thermal properties showed, that PUR-foam is a suitable material for transportation tanks for

cryogenic liquids. Considering the size of the small-scale tank prototype, the results for the boil-off rate and pressure-increasing-time are satisfying. With the tested insulation material and thickness, the goal of a maximum of 4 bar (relative) internal pressure seems achievable. However, this prediction needs to be confirmed in further experiments with tanks of different sizes.

Measuring the boil-off rate provides a simplified testing method compared to pressure testing. The exact relation of boil-off rate to increase in pressure needs to be analyzed. These experiments will deliver the possibility to generate information about the performance of a full-sized tank by examining a small-scale tank prototype.

The experiments on the mechanical properties showed a significant difference regarding the bending modulus and maximum stress of specimen in cryogenic three-point-bending-tests compared to tests at room temperature. This finding agrees to the information found in [7]. Up to approximately 30 MPa the bending modulus was at approximately 6.200 MPa for both, cryogenic and room temperature testing. At a higher load, it dropped by more than 50 % for cryogenic testing down to appr. 2.800 MPa. However, the maximum stress could not be reached at cryogenic conditions as it exceeded maximum displacement of the testing setup due to dimensional restrictions. These tests will be extended to reach the maximum stress. Furthermore, tests will be conducted in perpendicular direction as well. To examine the influence of temperature and moisture, samples will be conditioned in a dry room and wet air. Testing will be conducted at room temperature and cryogenic temperatures. Furthermore, the test setup will be modified and a cryogenic gas system will be installed for cooling the specimen. This allows other mechanical testing methods, such as tensile tests, as no liquid nitrogen is necessary for cooling.

Numerical models of both thermal and mechanical examinations will be realized to understand the ongoing effects at cryogenic temperature and to analyze different design options for the real-scale tank.

## Acknowledgements

We would like to thank our partners in this project from the Brandenburg University of Technology Cottbus-Senftenberg and VKA GmbH. We also would like to thank the AiF Projekt GmbH for financial support of this project (project number ZF4044213EB7).

## Keywords

Glass fiber reinforced polymer, cryogenic liquids, liquefied natural gas, transportation tanks.

Received: 10 June 2019

Revised: 22 July 2019

Accepted: 23 July 2019

## References

1. DIN Deutsches Institut für Normung e.V., DIN EN ISO 16903: Erdöl- und Erdgasindustrie - Eigenschaften von Flüssigerdgas mit Ein-uss auf die Auslegung und die Materialauswahl.
2. Rosenstiel, D.P.-v., LNG in Deutschland: Flüssigerdgas und erneuerbares Methan im Schwerlastverkehr, Deutsche Energie-Agentur GmbH (dena), 2015.

3. Chen, Q.S.; Prasad, V.; *Cryogenics*; **2004**, *44*, 701.
4. Holzhäuser, K.R.J.; Europäisches Übereinkommen über die internationale Beförderung gefährlicher Güter auf der Straße (ADR), Bundesamt für Strassen, **2019**.
5. Umrath, W.; Grundlagen der Vakuumtechnik, Leybold Vakuum, **1997**.
6. Kleiber, R. J. M.; VDI-Wärmeatlas, Stoffwerte und Zustandsgrößen, Verein Deutscher Ingenieure, VDI-Gesellschaft Verfahrenstechnik und Chemieingenieurwesen, **2006**.
7. Schürmann, H.; Konstruieren mit Faser-Kunststoff-Verbunden, Springer, **2007**.
8. W.C. Limited, ISO VAC 20 - LNG.
9. Fadzil, M.A.B.M.; Erstellen eines Berechnungsalgorithmus für einen Flüssiggastank während der Bereitschaftsphase, Hochschule Zittau/Görlitz, **2019**.
10. Geiss, G.; Einfluss von Tieftemperatur und Wasserstoff auf das Versagensverhalten von Glasfaser-Verbundwerkstoffen unter statischer und zyklischer Belastung, Universität Karlsruhe (TH), **2001**.
11. Bunker, T.A.M. B. C.; *Fracture mechanics of ceramics*; **1986**, *8*, 391.